Central Aerohydrodynamic Institute

TsAGI

**Zhukovsky, Moscow region, Russia**

" 10 " December 1999

Final report

Experimental Investigation of Supersonic Combustion of Liquid Hydrocarbon Fuel Using Barbotage in the Aeroramp Configuration at M=2.5

Principal Investigator   Vladimir Sabel'nikov

10. 12. 99

20000207 038

AQF00-05-1183

REPORT DOCUMENTATION PAGE

Form Approved OMB No. 0704-0188

1. AGENCY USE ONLY (Leave blank)	2. REPORT DATE 1999	3. REPORT TYPE AND DATES COVERED Final Report

4. TITLE AND SUBTITLE

Experimental Investigation Of Supersonic Combustion Of Liquid Hydrocarbon Fuel Using Barbotage In The Aeroramp Configuration at M=2.5

5. FUNDING NUMBERS

F61775-99-WE050

6. AUTHOR(S)

Dr. Vladimir Sabelnikov

7. PERFORMING ORGANIZATION NAME(S) AND ADDRESS(ES)

TsAGI
Zhukovsky St
Moscow 140160
Russia

8. PERFORMING ORGANIZATION REPORT NUMBER

N/A

9. SPONSORING/MONITORING AGENCY NAME(S) AND ADDRESS(ES)

EOARD
PSC 802 BOX 14
FPO 09499-0200

10. SPONSORING/MONITORING AGENCY REPORT NUMBER

SPC 99-4050

11. SUPPLEMENTARY NOTES

12a. DISTRIBUTION/AVAILABILITY STATEMENT

Approved for public release; distribution is unlimited.

12b. DISTRIBUTION CODE

A

13. ABSTRACT (Maximum 200 words)

This report results from a contract tasking TsAGI as follows: The contractor will investigate the following injection schemes 1) Inject through the first row of orifices of aeroramp (which are at the small angle to the mainstream air flow direction) air, but not kerosene is not to be used, since kerosene jets rested at the vicinity of the wall and as result were poorly mixed with air; 2) Change the fuel supply by variation of the impulse of kerosene jets which can be reached by varying the pressure and/or diameter of the orifices, angles of injection; 3) Installation of the aeroramps on upper and bottom walls of combustor. The tests are to be carried out at the hypersonic wind tunnel using direct-connect scheme. The tests will be performed using the same combustor, which was used for the tests during the 1st stage. Preparation of fuel is performed using the scheme of barbotage as the previous tests. Barbotage of kerosene will be carried out by air.

14. SUBJECT TERMS

EOARD, Combustion, Supersonic and Hypersonic Flows, Fuel Injection

15. NUMBER OF PAGES

50

16. PRICE CODE

N/A

17. SECURITY CLASSIFICATION OF REPORT	18. SECURITY CLASSIFICATION OF THIS PAGE	19. SECURITY CLASSIFICATION OF ABSTRACT	20. LIMITATION OF ABSTRACT
UNCLASSIFIED	UNCLASSIFIED	UNCLASSIFIED	UL

NSN 7540-01-280-5500

Standard Form 298 (Rev. 2-89)
Prescribed by ANSI Std. 239-18
298-102

Contents

Abstract

Results of investigations of combustion of liquid hydrocarbon fuel jets aerated by air in a supersonic flow in the two-dimensional diverging-area supersonic combustor are presented. Direct-connect combustor tests were conducted at the combustor entrance Mach number M=2.5 and total temperature in the range of Tt=1635-1742K. The liquid hydrocarbon fuel supply into the combustor was executed through the modified (in comparision with the baseline) aeroramp configurations : 1) installation of baseline aeroramps at the upper and bottom walls of the combustor, 2) combined fuel feed through injector nozzles of aeroramps separetely of air and of fuel aerated by air, 3) injectors with the different from baseline aeroramps angles of fuel injection and geometry nozzles. The results obtained with the modified aeroramp configurations are superior to earlier ones obtained with baseline aeroramp configuration.

1. Introduction

The second stage of the investigation of the supersonic mixing and combustion enhancement technique was initiated and supported by Air Force Office of Scientific Research (AFOSR) USA, contract F61775-98-WE118, SPC 98-4078. The investigations were done in cooperation with Dr. Th. Jackson and Dr. M. Gruber, and Dr. Ch.Raffoul, as the technical monitor.

The objective of the second stage was to study the efficiency of application of "aeroramp" configurations (gas wedges) to inject the liquid hydrocarbon fuel aerated by air for enhancement of the supersonic mixing and combustion. The following results were obtained [1]:

- The fuel supply through aeroramp - injectors forms in a supersonic flow wave structure similar to one around the wedge injector (in full correspondence with the supposition [2,3]).

- The fuel supply through aeroramp - injectors results in a quite large nonuniformities in vertical fuel distribution in the combustor duct with the maximum fuel concentration in the proximity of the wall at which aeroramps were installed.

- The aeroramp-injectors result in less intense combustion process in comparison with the tube-injectors.

- The aeroramp-injectors provide a larger domain of the stable combustion in comparison with the tube-injectors.

- Type of gas used for aeration of the liquid hydrocarbon fuel has a minor influence on the intensity of the mixing and combustion in the supersonic combustor.

The above results have shown clearly the necessity of the further research of aeroramp configuration. The evaluation of the earlier obtained results was made by

Dr. Th. Jackson and Dr. M. Gruber (by correspondence course), by Dr. Lee Bain and Dr. Ch. Raffoul during joint technical meeting which took place at TsAGI 13 July, 1999, Zhukovsky, Russia, devoted to the key results of work fulfilled in the frame of the contract F61775-98-WE118. They expressed also the expediency of the continuation of the research directed to improve the characteristics of aeroramp - injectors and technology of their application.

The main suggestions are as follows:

· To reach the better uniformity in vertical fuel distribution in the combustor duct at the expense of the installation of aeroramps at the upper and bottom walls of the combustor.

· To increase fuel jets penetration by changing hydrodynamical structure of the jets forming a gas wedge and, in particular, by using combined fuel feed through injector nozzles separately of air and of fuel aerated by air.

· To increase fuel jets penetration by choosing the different from baseline aeroramp angles of fuel injection (it is supposed to increase the angle of injection through separate injector nozzles and thus to change geometry of their mutual arrangement).

The aim of the present third stage of the work (which is done in the frame of the contract Contract F61775-99-WE050, SPC 99-4050, Air Force Office of Scientific Research (AFOSR), USA) is to study the supersonic mixing and combustion enhancement in the scramjet combustor using the liquid hydrocarbon fuel jets aerated by air in the modified aeroramp configurations (five variants with three kinds of aeroramps , including baseline ones).

The study was carried out at TsAGI test facility T-131B using the direct-connect tests. The intermediate results of the work were presented in the first interim report [4].

The final report summarizes the description of the test facility (paragraph 2), supersonic combustor model (paragraph 3), injectors (paragraph 4), tests

methodology and instrumentation (paragraph 5), results of tests, their analysis and discussions (paragraph 6). Conclusions are given in paragraph 7.

2. Experimental facility

The experimental investigation of combustion of liquid hydrocarbon fuel jets aerated by gas (air or hydrogen) was performed in the direct-connect facility of TsAGI T-131B. Kerosene-air vitiated heater with oxygen replenishment was used to provide the high enthalpy flow with the desired values of the stagnation pressure Pt and the stagnation temperature Tt and the mass fraction of free oxygen Y_{O2} (23%).

The kerosene combustion efficiency in the heater was close to 1. The estimates based on the results of numerical calculations show that the combustion products from the heater at $T_t \leq 2000$ K practically consist of CO_2, H_2O, N_2, O_2, i.e. there is no dissociation. A summary of the total flow parameters and other parameters characterizing the facility and combustor operation regimes are given in Table No.1.

Figure 1 shows the scheme of the facility and supersonic combustor. Kerosene was supplied into the heater through a two-dimensional fuel manifold equipped with rotary-type injectors (discharge nozzles) for spraying the liquid fuel.

The oxygen and air were supplied into the heater through the Venturi-type nozzles with the nozzle throat diameters of 7.5 and 14.4 mm, respectively. The choice of such sizes of the Venturi-type nozzles is specified by providing the oxygen mass fraction of 23% in the heater at the gas stagnation temperature Tt=1700 K.

To generate a supersonic flow at the combustor entry, a two-dimensional Mach 2.5 nozzle was used. The throat dimensions of the nozzle are 10.6 x 100 mm^2 and the exit section dimensions are 30 x 100 mm^2. The nozzle was designed by the method of characteristics for the Mach number M = 2.5, the ratio of specific heats used for calculations was taken equal 1.33. The constructions of the heater and nozzle are cooled by water.

3. Supersonic combustor

The schematic view of the combustor is shown in Fig. 2. The combustor duct consisted of 4 sections (6 segments) bolted together:

- the first was 150 mm long with the constant area section of 30 x 100 mm^2 (one segment);

- the second was 150 mm long with the divergence angle of 3.0 degree along the upper wall, exit cross-area section is 37.8x100 mm^2 (one segment);

- the third was 300 mm long with the divergence angle of 2.3 degree along the upper wall, exit cross-area section is 49.9x100 mm^2 (one segment);

- the forth was 450 mm long with the constant cross-area section of 49.9x100 mm^2 (3 segments, each of them 150 mm long).

The total length of the combustor was 1050 mm; the area-expansion ratio of the combustor was 1.67. The combustor is smoothly attached to the nozzle, since the cross-area section of the combustor duct entry coincides with the rectangular exit nozzle section with dimensions of 30x100 mm^2. The combustor cross-section (beginning from the distance 50 mm from the entrance section) has round corners; the radius of rounding is 5 mm. The combustor walls were uncooled, they are made of heat-resistant steel, the wall thickness is 8 mm. The combustion times during test runs did not exceed 6 seconds to avoid excessive wall temperatures.

The upper and lower walls of the combustor are drained by the holes (46 locations) for measuring the static pressure on the wall along the combustor with a spacing of 30 –50 mm.

At the upper wall there are also holes along the combustor duct for installation of heat flux sensors.

An exhaust diffuser (into which the vertical 5-point pitot pressure rake cooled by water was installed) can be attached to the last segment of the combustor. The last

segment of the combustor is equipped with a manifold (collector) for a normal injection of air jets into the combustor duct that allows us to perform the combustor flow throttling that is necessary for establishing conditions for the fuel ignition and combustor start.

The first combustor segment has a hatch on the upper wall and the second combustor segment has a hatch on the lower wall, dimensions of which are 80x90 mm^2. Different types of injectors for fuel supply can be installed at the hatch covers.

4. Injectors

Three kinds of aeroramp - injectors for supplying the liquid hydrocarbon fuel jets aerated by gas were investigated [1,4]:

- injectors of the baseline configuration mounted (in pairs) at the upper and bottom walls of combustor (variant I);
- injectors of the baseline configuration mounted at the upper wall of combustor (variant II);
- injectors with the different from baseline configuration angles of fuel injection and geometry nozzles (variant III);
- aeroramp - injectors with separate feed of nozzles by air (1-st row) and by fuel aerated by air (2-nd and 3-d rows), all others characteristics as for the baseline configuration (variant IV and V).

In the 1-st variant aeroramp - injectors (overall number 4 pieces) were mounted in one row at the distances of 95 mm and of 205 mm from the combustor entrance at the upper and bottom combustor walls, respectively, and 25 mm from the side walls. The installation scheme of the aeroramps at the cover and location of each of 9 holes-nozzles of the diameter d = 0.6 mm are presented in Fig.3.

In the 2-nd variant aeroramp - injectors (2 pieces) were mounted in one row at the distances of 95 mm from the combustor entrance at the upper combustor wall and

25 mm from the sidewalls. The geometry and scheme of the aeroramps are presented in Fig.4.

In the 3-d variant aeroramp - injectors (2 pieces) with the different from baseline configuration angles of fuel injection and geometry were mounted at the combustor walls as for the 2-nd variant. The geometry and scheme of the aeroramps are given in Fig.5.

In the 4-th and 5-th variant aeroramp - injectors (2 pieces) with separate feed of nozzles by air and by fuel aerated by air were mounted at the combustor walls as for the 2-nd variant. In the 4-th variant air supplied to the 1-st row and fuel to the 2-nd and 3-d rows. In the 5-th variant air supply to the 1-st row was small with respect 4-th variant (~ 10%). The geometry and scheme of the aeroramps are presented in Fig.6.

The liquid hydrocarbon fuel jets will be aerated by air with the mass fraction of gas $\leq$ 0.1.

5. Tests methodology and instrumentation

Test runs are performed in the following sequence:

- the data acquisition system is switched on;
- the air-heater is switched on and the required conditions with respect to the stagnation pressure P_t and temperature T_t are attained;
- the fuel supply into the combustor and also air for variants IV and V is included on the beforehand given regime by pressure and fuel rate;
- the kerosene-air mixture is ignited using an air jet pulse (0.5 - 1 s) through a flush wall injector located at the end combustor segment (pulsed combustor throttling);
- after ignition and reaching the steady combustion process the fuel supply is continued during 5 - 6 s;

- minimum fuel equivalence ratios ER at which the extinction of the flame take place (i.e. fuel lean blowout limit) were determined by continuous decreasing of the fuel rate.

During tests the following parameters are measured:

- pressure distributions at the combustor walls along the duct;

- heat fluxes to the combustor walls along the duct length;

- total pressure at the exit section;

- pressure in the fuel manifold and mass rate of fuel;

- pressure and temperature of oxygen before the Venturi tube;

- pressure and temperature of air before the Venturi tube;

- pressure and mass rate of kerosene before the fuel collector of the air-heater;

- pressure in the air-heater.

The scheme of measurements for the combustor model and the test facility, as well as the ranges, measuring devices are given in Fig.7.

During tests the video of burning of fuel on the exit of the combustor is carried out.

Visualization of the flow patterns and of fuel sprays in the supersonic flow at the combustor exit is done by the use of two videosystems: schlieren system in the horizontal plane and the colour video-system in vertical plane. The injectors are mounted at the special stand at the exit of the combustor.

6. Test results

Nine test runs were performed (see Table No.1). Test runs No.1 and No.9 were conducted with aeroramp-type injectors (overall number is 4 injectors) mounted in one row at the distances of 95 mm and of 205 mm from the combustor entrance at the upper and bottom combustor walls. In the test run No.9 the vertical total pressure rake was installed at a distance of 1050 mm from the combustor entrance.

Test run No.2 was conducted with injectors of the baseline configuration mounted at the upper wall of combustor.

Test runs No.3, 4 and No.5 were conducted with modified injectors mounted at the upper wall of combustor (variants III, IV and V).

In test runs No.6, 7 and No.8 visualization of the liquid hydrocarbon fuel jets aerated by air and injected through the aeroramp-injectors was performed without combustion (Fig.24–26). Fuel rates through injectors were 20, 23.5 and 28 g/s for variants III, IV and V, respectively. The relative fuel rate (respectively to the fuel rate through nozzles) was 0.2 for variant IV. The injectors were installed at the combustor exit at the distance of 900 mm from the combustor entrance, ensuring the possibility to perform the visualization in the free flow.

Figs.8 and 9 show the axial normalized pressure (the ratio of the static pressure to the heater pressure) distributions on the combustor walls for the baseline injectors mounted at the upper and bottom combustor walls in the test run No.1.

Fig.10 show the normalized static pressure distributions along the combustor walls for the test run No.2 for the injectors with baseline configuration mounted at the upper wall of combustor.

Figs.11 and 12 shows the axial normalized pressure distributions on the combustor walls for the injectors with the different from baseline configuration angles of fuel injection and geometry nozzles mounted at the upper combustor wall (test run No.3).

Figs.13-16 show the axial normalized pressure distributions on the combustor walls for the injectors with separate feed of nozzles by air and by fuel mounted at the upper combustor wall (test runs No.4 and No.5).

The total pressure measurements at the distance of 1050 mm from the entrance, presented in Fig.17 (which were carried out by means of the rake), show that a practically uniform flow occurred in the test run No.1.

The heat flux distributions measured along the upper wall of the combustor in the test runs No.1-No.5 are presented in Figs.18-22. From the heat flux distributions to the walls of the divergent part of it is seen that the heat flux magnitudes are considerably large for upper wall than for bottom wall (see Figs.10, 11 in report [1]): q_w=2.3-2.5x10^6 and q_w=1.3-1.7x10^6 W/m^2 for upper and bottom walls, respectively.

The estimation of the efficiency of the combustion and mixing of the liquid hydrocarbon fuel jets aerated by gas was carried according to the increment of the axial component of the integrated inner pressure force and the combustion efficiency (see details in [6,7]). The increment of the axial component of the integrated inner pressure force was determined from the measured (with and without combustion) static pressure distributions using the following relationship:

$$\Delta F = w \int (P_{comb} - P_{nocomb}) tg\theta dx, \qquad (1)$$

$$\Delta \overline{\mathcal{F}} = \Delta \mathcal{F} / I_1,$$

$$I_1 = (P + \rho V^2) hw,$$

where θ is the local wall angle with respect to the flow direction, x is the axial coordinate, w is the duct width, $I_1 = (P + \rho V^2) hw$ is the total gasdynamic impulse at the combustor entrance.

Further analysis of the investigation results took into the account the estimated combustor efficiency (mixing and burning) concerning the level of pressure

increment along the combustor, relative increment of axial component of the integrated inner pressure force on the combustor walls, changing of the thermal flows level, burning efficiency ratio on 900 mm from the combustor inlet. Qualitative evaluation of the injectors in a specific combustor was also made on the basis of the analysis of conditions under which the extinction of the flame occurs.

Comparative analysis of the test runs results No.1 and 2 (variants I and II) show that when the fuel is supplied through baseline configuration injectors from two opposite walls with burning fuel then the flow field becomes more uniform on the exit of the combustor (fig. 17) compared to the one-side fuel supply (Fig.12 in report [1]). The increment of the axial component of the integrated inner pressure force ($\Delta \overline{F}$) for variant I and ER=0.52 is 20% larger, than with one side fuel supply (see Fig. 27, 28, 30 and Tab. No.2). The extinction of the flame for variant I takes place with ER=0.346 (Fig.9), while for baseline variant II it occurs when ER=0.33 [1].

For one side fuel supply through injectors with the increased angles of nozzles installed in 2-nd and 3-d rows (variant III) the increment of the axial component of the integrated inner pressure force is also larger and equals to 18% for ER≈0.5 (Fig.28). The extinction of the flame for variant III takes place with ER=0.358 (Fig.12).

Injectors with separate feed of nozzles by air (1-st row) with a relative air flow rate ≤ 0.2 and with fuel supply through 2-nd and 3-d rows (variant IV) with ER≈0.5 provide an extra increment of the axial component of the integrated force by 30-35% (when burning) compared to the baseline injectors (Fig. 29, 30). The extinction of the flame for variant IV takes place with ER=0.365 (Fig.14).

Injectors with separate feed of nozzles by air (1-st row) with a relative air flow rate ≤ 0.02 and with fuel supply through 2-nd and 3-d rows (variant V) with ER≈0.5 provide an extra increment of the axial component of the integrated force by 20% (when burning) compared to the baseline injectors (Fig. 29). The extinction of the

flame for variant V takes place with ER=0.361 (Fig.16).

The figure 30 presents the normalized increments of the axial component of the integrated inner pressure force $\Delta \overline{F}$ induced by the combustion (for the all variants).

From Fig.30 it is seen that the $\Delta \overline{F}$ increases with the growth of the ER and for the modified injectors it is considerably higher than for the baseline injectors.

The combustion efficiency was calculated by using a one-dimensional methodology [5] based on the solution of the equations of energy, mass and momentum conservation at the known experimental values of the pressure distribution along the combustor walls (pressure was assumed to be constant across the duct section). The calculated combustion efficiency and mass-averaged flow parameters Mach number M and total pressure losses σ for the section at the distance of 900 mm from the combustor entrance are given in Table No.2.

7. Conclusions

The experimental study of the combustion of the liquid hydrocarbon fuel jets aerated by air were performed in the two-dimensional diverging-area supersonic combustor with the use of three kinds of modifications of baseline aeroramp - injectors. The experiments were performed with the following flow parameters at the combustor inlet: Mach number M=2.5, the stagnation temperature Tt=1635-1742 K, stagnation pressure Pt=1.8-1.84 MPa, the mass fraction of free oxygen Y_{O2} = 0.216-0.235, ER=0.343-0.65. The following results were obtained:

1- The fuel supply through the injectors of the baseline configuration mounted (in pairs) at the upper and bottom walls of combustor gave a more uniform vertical fuel distribution in the combustor duct and increase the combustion efficiency.

2- Investigated schemes of the injectors (the variants I, III, IV, V) in comparison with baseline scheme (the variant II) produced a larger increment of the axial component of the integrated inner pressure force.

3- Combustion efficiency varies greatly depending on positioning of the nozzles in injectors as well as on the distribution of fuel and air supply along the rows.

4- The extinction of the flame for the injectors investigated (except the variant II) take place in the range ER=0.346-0.365.

References

1. V.A. Sabel'nikov et al. Experimental Investigation of Supersonic Combustion of Liquid Hydrocarbon Fuel Using Barbotage in the Aeroramp Configuration at M=2.5. Final report on Contract F61775-98-WE118, SPC 98-4078, Air Force Office of Scientific Research (AFOSR), USA, 1999.

2. P. Clement, C. Rodriguez. Shock wave structure and penetration height in transverse jets. AIAA Paper 89-0841, 1989.

3. J.M. Tishkoff, J.P .Drummond, T.E. Edvards and A.S. Nejad. Future directions of supersonic combustion research: Air Force / NASA Workshop on Supersonic Combustion. AIAA Paper 97-1017 35th AIAA Aerospace Sciences Meeting @ Exhibition, Jan. 1997.

4. V.A. Sabel'nikov, V.V. Ivanov, Experimental Investigation of Supersonic Combustion of Liquid Hydrocarbon Fuel Using Barbotage in the Aeroramp Configuration at M=2.5 1st quarterly report on Contract F61775-99-WE050, SPC 99-4050, Air Force Office of Scientific Research (AFOSR), USA, 1999.

5. V.A. Sabel'nikov et al. Investigation of Supersonic Combustion Enhancement Using Barbotage and Injectors with Noncircular Nozzles. Final report on Contract NAVY USA ONR 000014-96-1-0869, 1997.

6. V.A. Sabel'nikov et al. Investigation of supersonic combustion enhancement using barbotage and injectors with noncircular nozzles. AIAA Paper 98-1516, p.10, 1998.

7. Scott D. Stouffer, Uri Vandsburger, G.Burton Northam. Comparison of Wall Mixing Concepts for Scramjet Combustors, AIAA Paper 94-0587, p.12, 1994.

Table No1. Tests conditions

Run number	P_t, MPa	T_T, k	Y_{O2}	ER	P_{mix}, MPa
Injector-aeroramp (variant 1)					
1	1.83	1716	0.227	0.656	1.652
	1.82	1696	0.229	0.521	1.243
	1.81	1714	0.216	0.424	0.974
	1.8	1635	0.23	0.368	1.155
	1.81	1646	0.235	0.346	1.172
	1.81	1651	0.232	0.343	1.11
	1.81	1726	0.227	0	-
9*	1.82	1696	0.229	0.521	1.243
	1.82	1702	0.236	0	-
Injector-aeroramp (variant 2)					
2	1.81	1691	0.232	0.576	3.556
	1.81	1698	0.226	0.508	3.435
	1.8	1677	0.229	0.42	3.11
	1.81	1689	0.231	0	-
Injector-aeroramp (variant 3)					
3	1.8	1705	0.231	0.641	3.795
	1.8	1700	0.229	0.507	3.335
	1.82	1678	0.234	0.417	3.267
	1.82	1683	0.226	0.391	3.046
	1.81	1663	0.23	0.358	2.955
	1.81	1678	0.235	0.352	2.923
	1.81	1720	0.227	0	-
6**	2.55	1450	0.27	-	3.0
Injector-aeroramp (variant 4)					
5	1.81	1679	0.232	0.548	4.356
	1.81	1676	0.23	0.507	4.203
	1.81	1670	0.23	0.42	3.815
	1.82	1698	0.231	0.385	3.676
	1.82	1706	0.228	0.365	3.559
	1.82	1704	0.231	0.354	3.542
	1.81	1681	0.23	0	-
7**	2.58	1500	0.26	-	3.5
Injector-aeroramp (variant 5)					
7	1.84	1742	0.228	0.541	4.381
	1.83	1720	0.229	0.502	4.195
	1.83	1717	0.229	0.417	3.8
	1.82	1716	0.229	0.379	3.773
	1.82	1716	0.23	0.361	3.664

		1.81	1698	0.23	0.355	3.6
		1.82	1711	0.228	0	-
	8**	2.55	1480	0.27	-	3.7

* - run with rake at X=900 mm section from combustion entrance

** - run with visualization of jets

Y_{O2} – oxygen mass fraction in heater gas ER – equivalence ratio
Pmix – pressure of injection
Y_{bar} – barbotage mass frection (G_{gas} / G_{sum})

Table No2. Flow parameters at the distance x=900 mm from the combustor entrance

RUN	ER	η	σ	M
Variant I				
1	0.656	0.963	0.363	1.06
-"-	0.521	0.952	0.351	1.07
-"-	0.424	0.940	0.346	1.17
-"-	0.368	0.969	0.341	1.15
-"-	0.346	0.770	0.358	1.32
Variant II				
2	0.576	0.935	0.356	1.07
-"-	0.508	0.920	0.349	1.09
-"-	0.42	0.862	0.338	1.12
Variant III				
3	0.641	0.941	0.359	1.02
-"-	0.507	0.944	0.351	1.09
-"-	0.417	0.914	0.336	1.06
-"-	0.391	0.864	0.341	1.19
-"-	0.358	0.843	0.342	1.23
Variant IV				
4	0.548	1.0	0.321788	1.06
-"-	0.507	0.991	0.315164	1.08
-"-	0.42	0.921	0.302199	1.10
-"-	0.385	0.910	0.299224	1.13
-"-	0.365	0.852	0.299005	1.20
Variant V				
5	0.541	1.0	0.354	1.07
-"-	0.502	0.979	0.351	1.10
-"-	0.417	0.902	0.336	1.10
-"-	0.379	0.891	0.336	1.18
-"-	0.361	0.708	0.354	1.35

Figure captures

Fig.1 Scheme of the test facility.

Fig.2 Schematic view of the model combustor.

Fig.3 Installation scheme of the aeroramps at the cover (variant I).

Fig.4 Scheme of the aeroramp-injectors (baseline, variant II).

Fig.5 Scheme of the modified aeroramp-injectors (variant III).

Fig.6 Scheme of the modified aeroramp-injectors (variant IV,V).

Fig.7 Scheme of measurements for the combustor and test bed.

Fig.8 Wall pressure distributions along the combustor (RUN No.1).

Fig.9 Wall pressure distributions along the combustor for modes of burning and blowout (RUN No.1).

Fig.10 Wall pressure distributions along the combustor (RUN No.2).

Fig.11 Wall pressure distributions along the combustor (RUN No.3).

Fig.12 Wall pressure distributions along the combustor for modes of burning and blowout (RUN No.3).

Fig.13 Wall pressure distributions along the combustor (RUN No.4).

Fig.14 Wall pressure distributions along the combustor for modes of burning and blowout (RUN No.4).

Fig.15 Wall pressure distributions along the combustor (RUN No.5).

Fig.16 Wall pressure distributions along the combustor for modes of burning and blowout (RUN No.5).

Fig.17 The total pressure profile at the combustor exit section (RUN No.9).

Fig.18 Heat flux distribution along the upper combustor wall (RUN No.1).

Fig.19 Heat flux distribution along the upper combustor wall (RUN No.2).

Fig.20 Heat flux distribution along the upper combustor wall (RUN No.3).

Fig.21 Heat flux distribution along the upper combustor wall (RUN No.4).

Fig.1.

1. pressure sensor
2. oxygen mixture
3. Venturi tube
4. mass rate metter
5. air-heater
6. injectors
7. aerator
8. throttling injector
9. fuel collector

Fig. 2.

air

148 | 148 | 148 | 300 | 150 | 150

$\vartheta = 2.3°$

$\vartheta = 3°$

fuel

fuel

205

95

30x100

Fig.3

NN	α	β
1	15	0
2	15	0
3	15	0
4	30	-15
5	30	0
6	30	+15
7	45	-30
8	45	0
9	45	+30

∅ 0,6 мм

flow direction

fuel

Fig.4

NN	α	β
1	15	0
2	15	0
3	15	0
4	45	-15
5	45	0
6	45	+15
7	80	-30
8	80	0
9	80	+30

β

Ø 0,6 мм

11.5

5

1.1

1.4

1.7

7 8 9

4 5 6

1 2 3

flow direction

α

fuel

65

54

20

50

20

Fig.5.

NN	α	β
1	15	0
2	15	0
3	15	0
4	30	-15
5	30	0
6	30	+15
7	45	-30
8	45	0
9	45	+30

⌀ 0,6 мм

flow direction

fuel

air
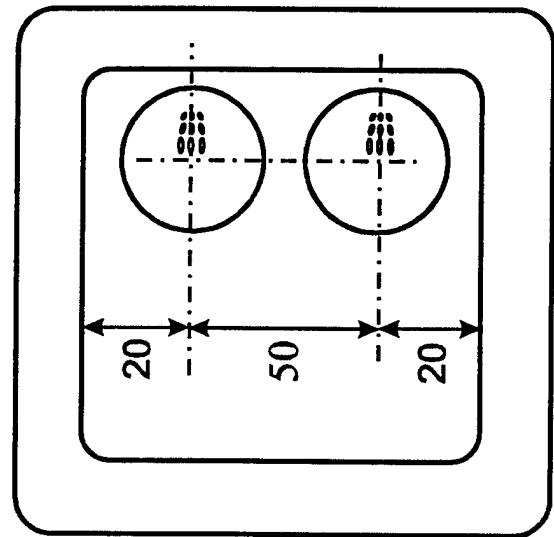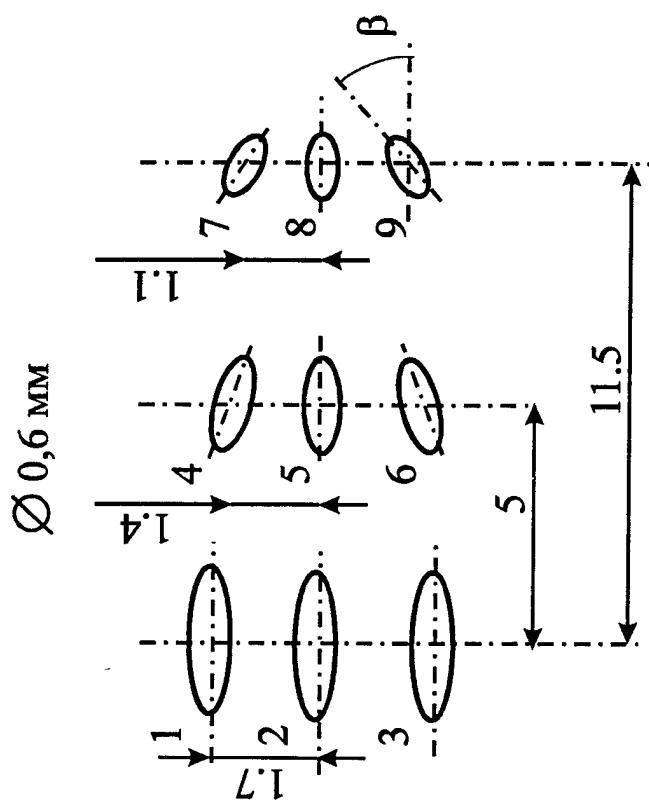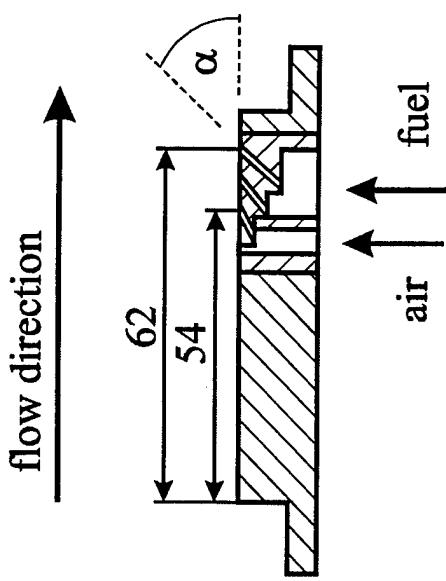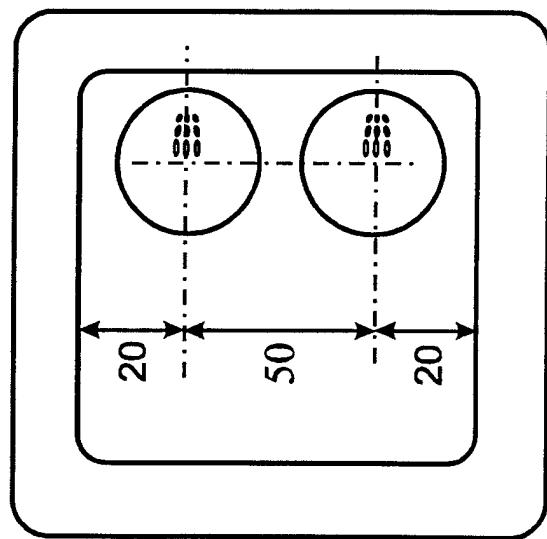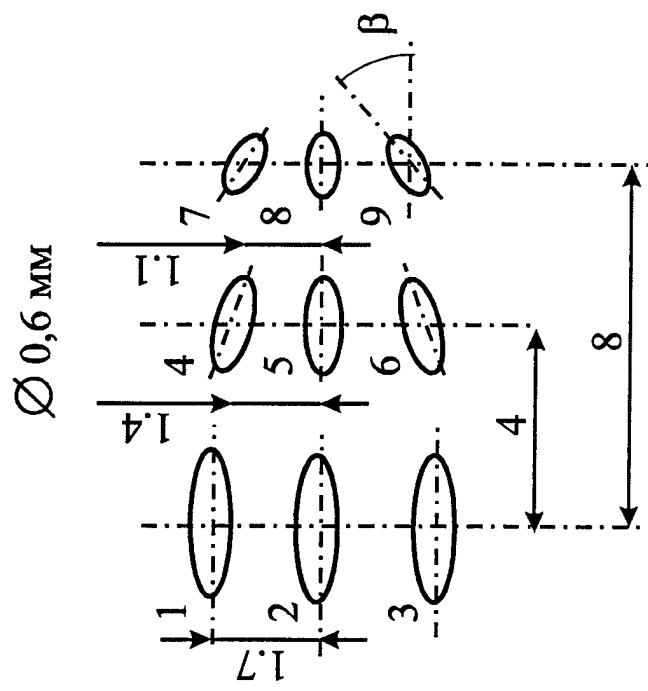
Fig.6
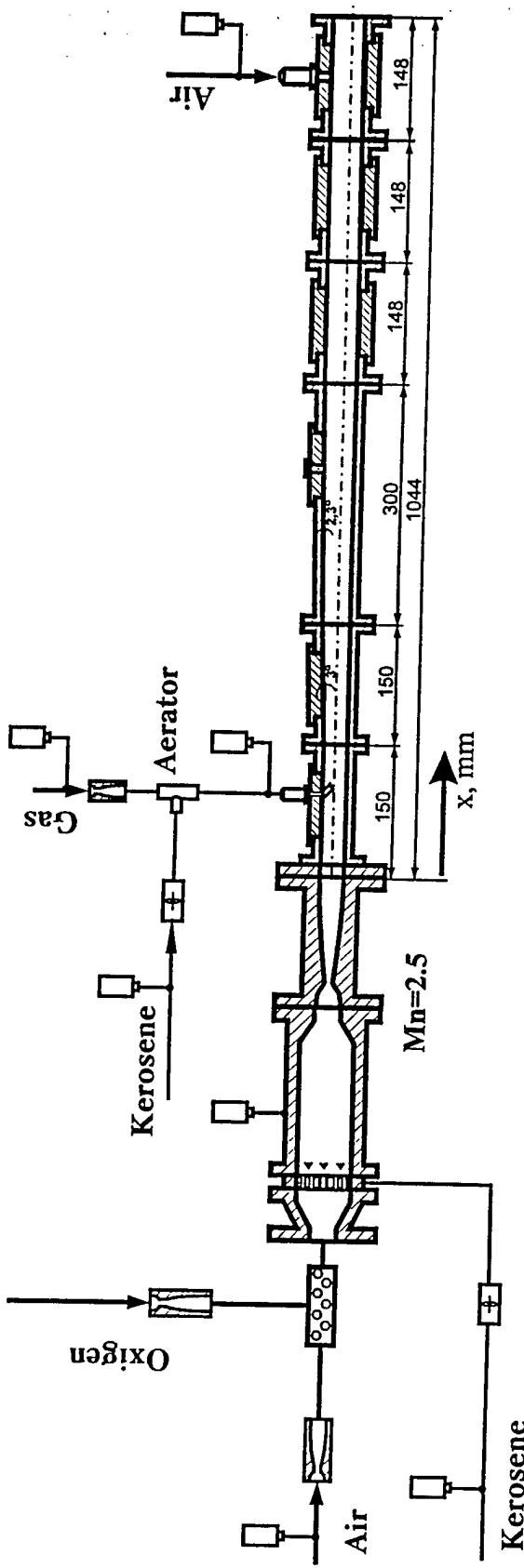
Fig. 7

heat flux sensors

Number of measurement point	1	2	3	4
distance from the nozzle exit, mm	75	260	420	570

bottom wall

pressure sensors

Number of measurement point	1	2	3	4	5	6	7	8	9	10	11	12	13	14	15	16	17	18	19	20	21	22	23	24	25	26
distance from the nozzle exit, mm	30	60	90	120	180	210	240	270	330	360	390	420	450	480	510	540	570	644	674	704	792	822	852	946	996	1039

bottom wall

Number of measurement point	27	28	29	30	31	32	33	34	35	36	37	38	39	40	41	42	43	44	45	46
distance from the nozzle exit, mm	37	55	55	60	65	70	80	95	180	210	240	330	360	390	420	570	792	822	852	894

upper wall

RUN N1

Pt,MPa	Tt,K	ER
1.81	1726	0
1.83	1716	0.656
1.82	1696	0.521
1.81	1714	0.424
1.81	1646	0.346

P/Pt

0.20
0.15
0.10
0.05
0.00

1200 x, mm

fuel

fuel

M=2.5

Fig. 8

Fig. 9

RUN N1

	Pt, MPa	Tt, K	ER
○ ●	1.81	1726	0
△ ▲	1.80	1635	0.368
⊠ ⊞	1.81	1646	0.346
☆ ★	1.81	1651	0.343

P/Pt

0.20

0.15

0.10

0.05

0.00

1200 x, mm

fuel

fuel

M=2.5

P/Pt

0.20

0.15

0.10

0.05

0.00

RUN N2

Pt, MPa	Tt, K	ER
1.81	1689	0
1.81	1691	0.576
1.81	1698	0.508
1.80	1677	0.420

○ □ ◇ ☆

● ■ ◆ ★

fuel

1200 x, mm

M=2.5

Fig.10

Fig.11

The figure contains the following legend:

RUN N3

	Pt, MPa	Tt, K	ER
○ ●	1.80	1720	0
□ ■	1.80	1705	0.641
◇ ◆	1.80	1678	0.507
☆ ✶	1.80	1658	0.417
⊠ ⊞	1.81	1663	0.358
△ ▲	1.81	1678	0.352

P/Pt

0.20 0.15 0.10 0.05 0.00

1200 x, mm

fuel

M = 2.5

Fig. 12

The figure contains a plot of P/Pt versus x, mm for RUN N3, with the following legend:

		P, MPa	Tt, K	ER
○	●	1.80	1720	0
☆	★	1.82	1678	0.417
◇	◆	1.82	1683	0.391
⊠	⊞	1.81	1663	0.358
△	◀	1.81	1678	0.352

P/Pt axis: 0.20, 0.15, 0.10, 0.05, 0.00

x, mm axis: 1200

M=2.5

fuel

RUN N4

	Pt, MPa	Tt, K	ER
○	1.81	1681	0
△	1.81	1679	0.548
◇	1.81	1676	0.507
□	1.81	1670	0.420
☆	1.82	1706	0.365
⊠	1.82	1704	0.354
●			
◄			
◆			
■			
★			
⊞			

P/Pt

0.20

0.15

0.10

0.05

0.00

fuel

1200 x, mm

M = 2.5

Fig.13

P/Pt

0.20

0.15

0.10

0.05

0.00

1200 x, mm

fuel

M=2.5

Fig.14

Fig.15

Fig.16

Fig.17

Fig.18

RUN N2

	Pt, MPa	Tt, K	ER
○	1.81	1689	0
●	1.81	1698	0.508

q /10⁶
$q/10^6$
w/m²
W/m²

2.00

1.00

0.00

M=2.5

fuel

1200 x, mm

Fig.19

Fig.20

Fig.21

RUN N5

	Pt, MPa	Tt, K	ER
○	1.82	1711	0
●	1.83	1720	0.502

q /10^6

wt/m²
Wt/m²

2.00

1.00

0.00

M=2.5

fuel

1200 x, mm
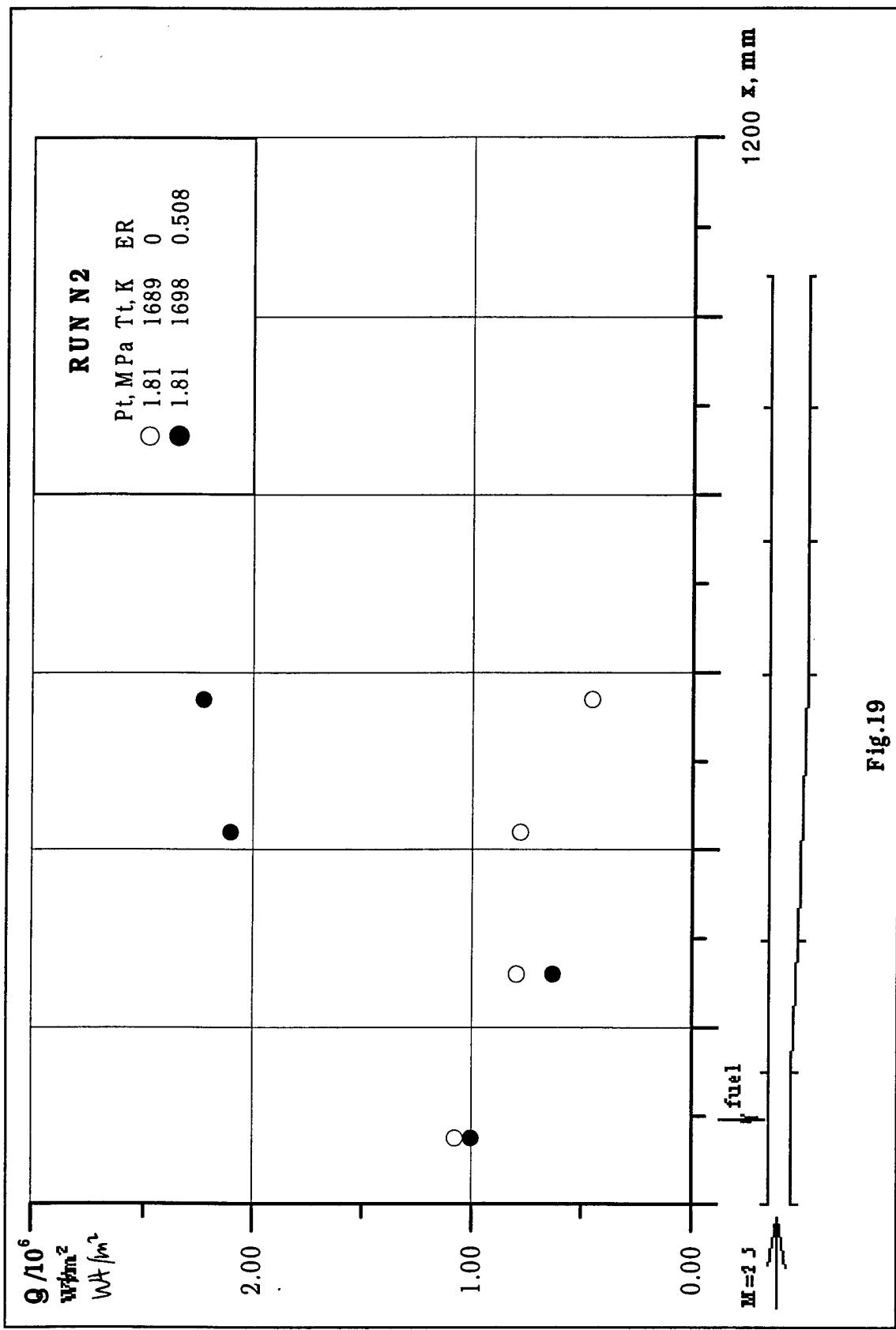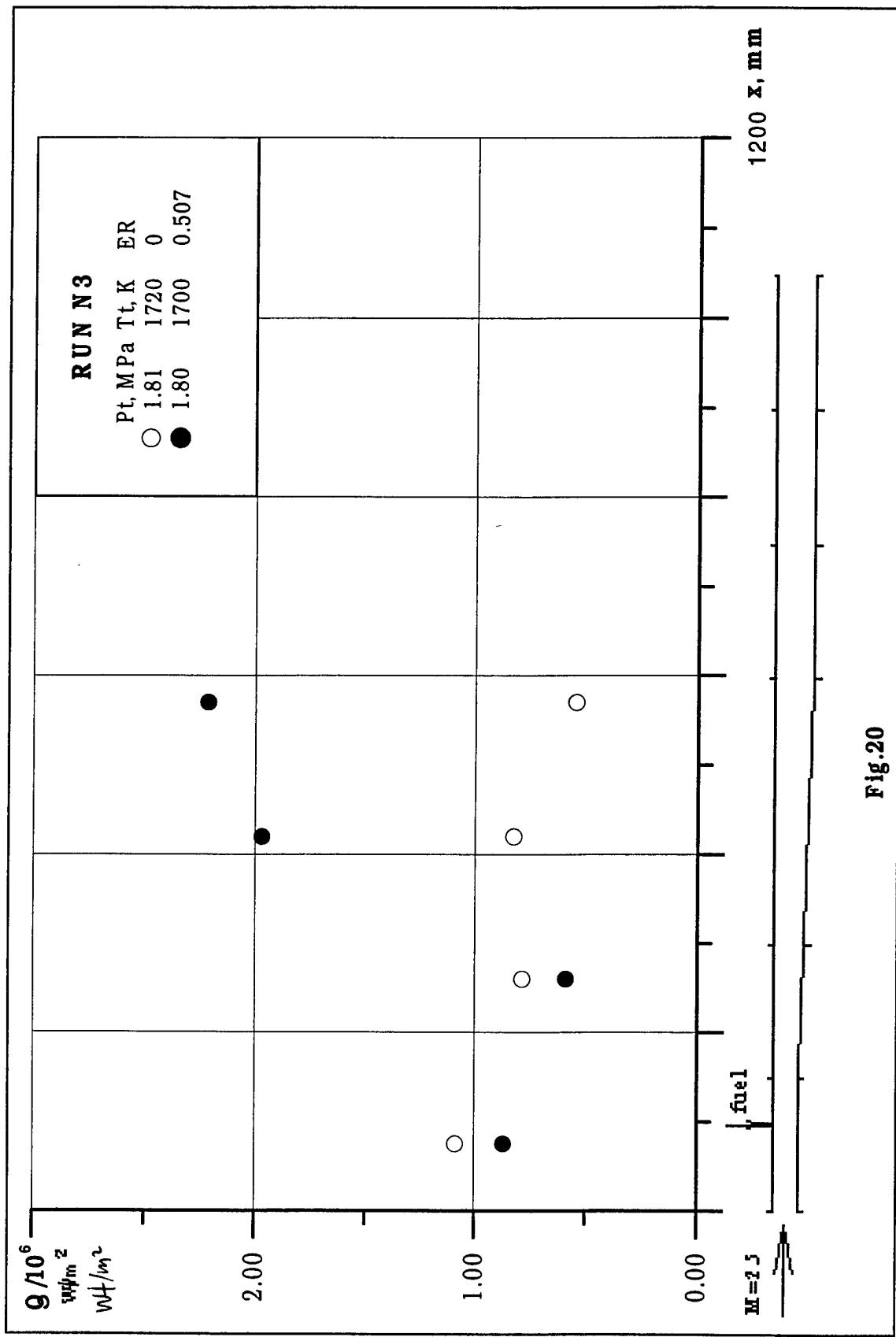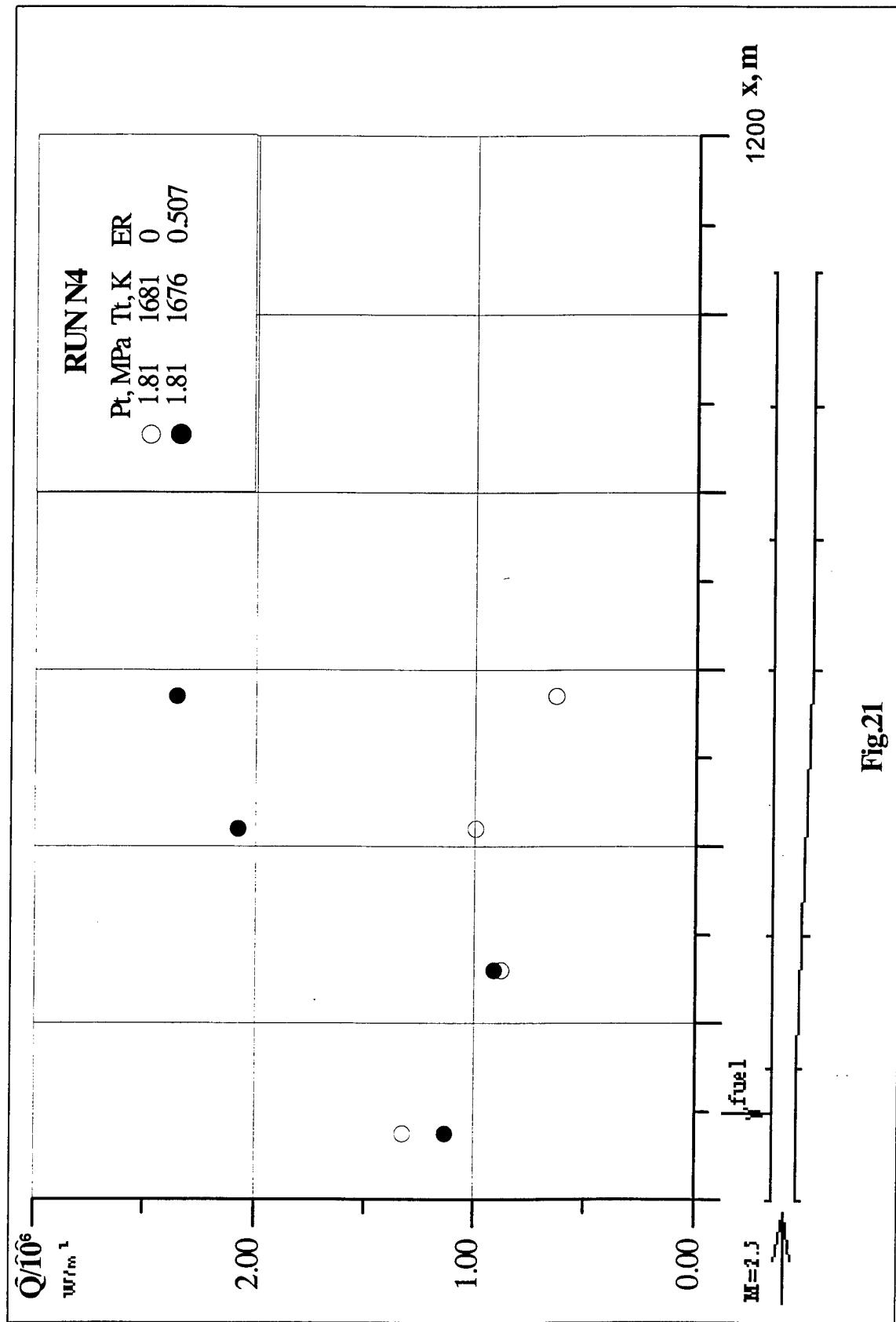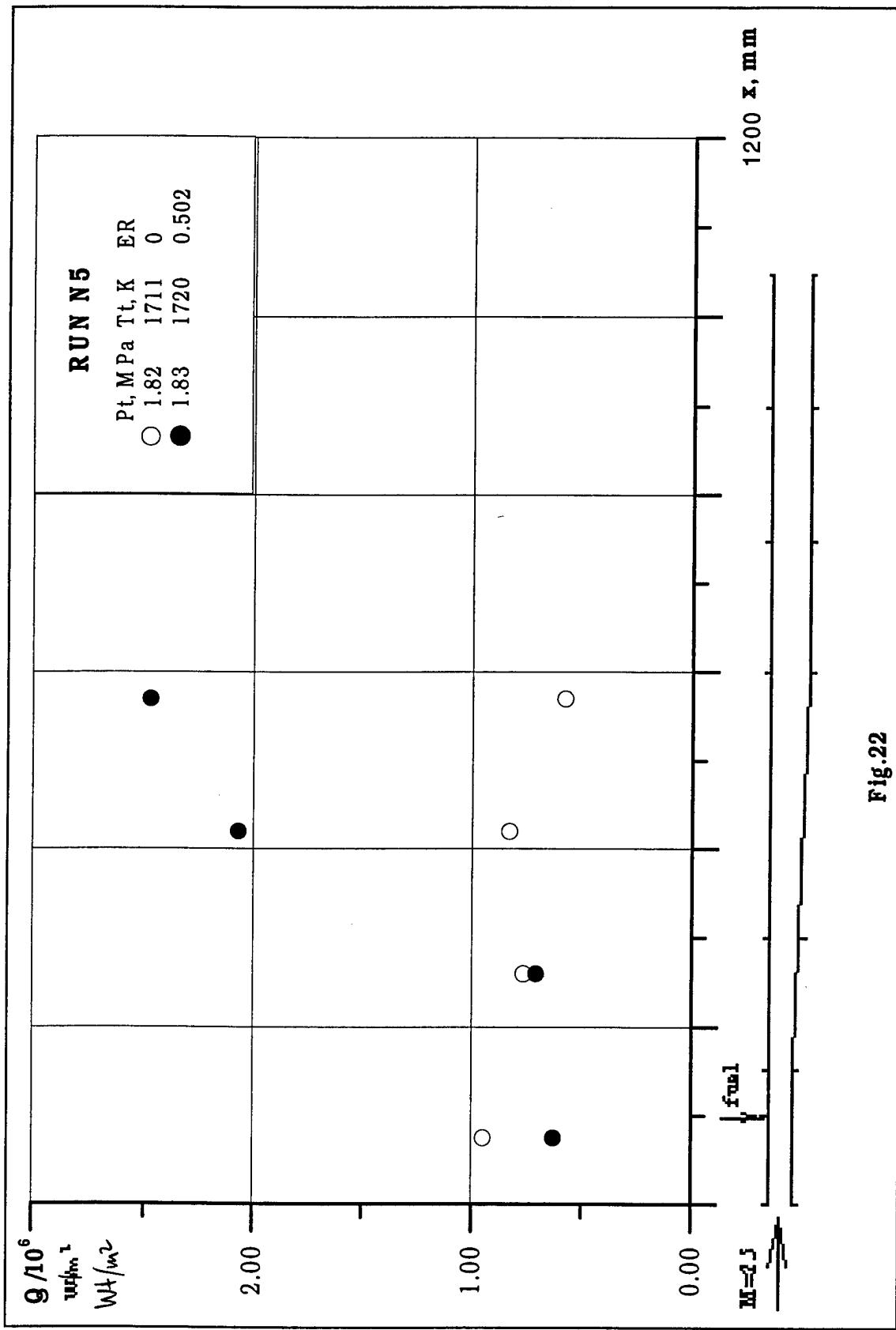
Fig.22

Variant II (baseline)

50 mm

Fig.23

Variant III

50 mm

Fig.24

Variant IV

50 mm

Fig.25

Variant V

50 mm

Fig. 26

Fig.27

Fig.28

Fig.29

The figure legend (table) reads:

Pt,MPa	Tt,K	ER	var.
○ 1.81	1681	0	-
△ 1.80	1687	0.420	II
☆ 1.81	1670	0.420	IV
⊠ 1.83	1717	0.417	V
● ◀ ★ ⊞			

Axis labels: P/Pt (vertical): 0.20, 0.15, 0.10, 0.05, 0.00
Horizontal axis: 1200 x, mm
M=2.5
fuel

Fig. 30

legend:
- variant I — ●
- variant II — ◆
- variant III — ■
- variant IV — ◀
- variant V — ★

axes: $\overline{\Delta F}$ (vertical, 0.00 to 0.12), ER (horizontal, 0.30 to 0.70)